

---

# FINDING BETTER PRECODING IN MASSIVE MIMO USING OPTIMIZATION APPROACH

---

A PREPRINT

Evgeny Bobrov<sup>1,2</sup>Dmitry Kropotov<sup>2,3</sup>Sergey Troshin<sup>3</sup>Danila Zaev<sup>1</sup>

July 29, 2021

**ABSTRACT**

The paper studies the multi-user precoding problem as a non-convex optimization problem for wireless MIMO systems. In our work, we approximate the target Spectral Efficiency function with a novel computationally simpler function. Then, we reduce the precoding problem to an unconstrained optimization task using a special differential projection method and solve it by the Quasi-Newton L-BFGS iterative procedure to achieve gains in capacity. We are testing the proposed approach in several scenarios generated using Quadriga – open-source software for generating realistic radio channel impulse response. Our method shows monotonic improvement over heuristic methods with reasonable computation time. The proposed L-BFGS optimization scheme is novel in this area and shows a significant advantage over the standard approaches.

**Keywords:** Optimization, Massive MIMO, Precoding

**1 Introduction**

The Multi-User MIMO system is an essential technology in modern wireless telecommunications [1]. It allows using antenna array clusters to send multiple signal beams for multiple user devices simultaneously. The proper construction of such beams is called *beamforming* or *precoding* procedures. In the linear channel assumptions, the correct precoding is a complex matrix of the general form with given constraints on its rows, which corresponds to the physical limitations of the system. We measure the quality of the final precoding using the common functionals such as Signal-to-Interference-and-Noise Ratio (*SINR*) and Spectral Efficiency (*SE*) [2].

Wireless channels with multiple inputs and multiple outputs (MIMO) provide significantly more bandwidth than their counterparts with one input and one output. In this article, we will investigate the case when one transmitter (base station) sends data to several receivers (users). Precoding is the process of using this information on a transmitter in such a way as to reduce multi-user interference.

We constrain ourselves to the case of linear processing on both the transmitter and the receiver. For the case when each user has only one receiving antenna, the optimal linear schemes for MMSE were derived in the papers [3, 4]. In this paper, we investigate a more complex case with several antennas per user. There are well-known methods of block diagonalization (BD) [5] and sequential MMSE (S-MMSE) [6]. Both have relatively low complexity but do not reach the minimum amount-MSE. Hence, we proceed to obtain a set of necessary conditions for the MMSE solution, which was presented in a similar form in [7]. The necessary conditions can be used to obtain an iterative approximation of the MMSE solution, an idea also used in [8]. However, the non-convexity of the objective function implies that this scheme ("direct optimization") does not always converge to a true MMSE solution. This problem can be partially solved by choosing a good initial assumption for the numerical algorithm. In [9, 10, 11], the duality between the problem under

---

<sup>1</sup>Huawei Russian Research Institute

<sup>2</sup>M. V. Lomonosov Moscow State University

<sup>3</sup>National Research University Higher School of Economics

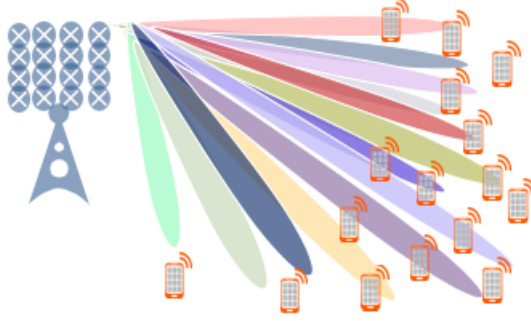


Figure 1: The MIMO wireless system allows to transmit different information to different users simultaneously.

consideration and the equivalent uplink channel is used to obtain an iterative algorithm that determines the true MMSE solution in each case.

The standard precoding algorithms, which are well-known in the literature, are Maximum-Ratio Transmission (MRT) [12], Zero-Forcing (ZF) [13] and Regularized Zero-Forcing (RZF) [14]. All these algorithms use analytical formulas, not taking into account the target functional of  $SE$  or do it implicitly, maximizing the numerator of  $SINR$  using the MRT algorithm, or reducing the denominator of  $SINR$  using the ZF algorithm [12, 13]. This leads to simple but non-optimal precoding solutions.

In this work, we reduce the precoding problem to an unconstrained optimization task and solve it by the full gradient-based method [15]. Using automatic differentiation in Pytorch-library [16] we can write an end-to-end differentiable projection-based method, where gradients are taken both for the functional and the projection, which tends to very fast convergence of the method. The problem is not convex, and so we find the local maximum of the *Spectral Efficiency*.

All investigated algorithms were tested in several scenarios of Quadriga version 2.4 [17] - open-source software for generating realistic radio channel impulse response. Our method shows monotonic improvement over heuristic methods with reasonable computation time.

The paper is organized as follows. Section 2 describes the research goals and achievements. In Section 3 we describe the system model of the Massive MIMO network and introduce all necessary notations. Section 4 contains the baseline precoding method on which we compare our method. In Section 5 we consider finding a precoding matrix using an optimization algorithm. Here we first introduce a proxy for spectral efficiency value that is fast to calculate and present an optimization algorithm that directly solves the main optimization problem. Then we introduce a fast version of the presented optimization algorithm that allows finding precoding matrix in time comparable to zero-forcing baselines. Section 6 shows the numerical results in the Quadriga channel simulator. Section 7 contains the conclusion.

We adopt commonly used notational conventions throughout the paper. Matrices and vectors will be denoted by bold-face upper and lower case letters, respectively. Furthermore,  $(\cdot)^H$  denotes Hermitian transpose.

## 2 Research Goals

The main goals of the project are the following:

1. Find a fast algorithm for calculating precoding matrix with better Spectral Efficiency values (6) comparing to linear Zero-Forcing baselines;
2. For a given precoding matrix algorithm find a fast algorithm for estimating a Spectral Efficiency value without direct calculation of the detection matrix inversion (2), (3).

Finally, in this study, we carried out:

1. We approximate the objective function of the spectral efficiency (6) using a computationally simpler function called "Conjugate Spectral Efficiency" (13) based on "Conjugate Detection" matrix (10);
2. Then, we reduce the precoding problem to an unconstrained optimization task and solve it by the Quasi-Newton L-BFGS iterative procedure to achieve capacity gains.

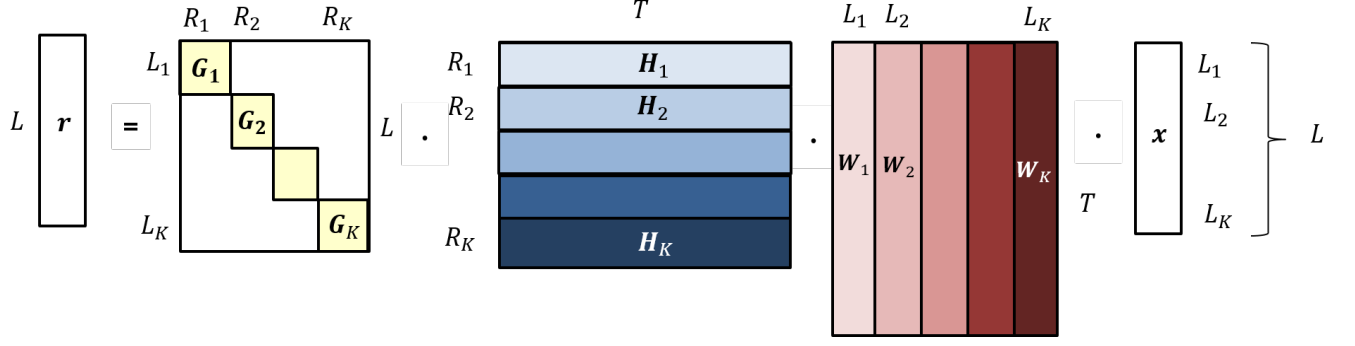


Figure 2: Multi-User Precoding allows to transmit different information to different users simultaneously. The problem is to find an optimal precoding matrix  $\mathbf{W}$  of the system given the target  $SE$  function.

### 3 System Model

We consider a precoding problem in multi-user massive MIMO communication in 5G cellular networks. Here a base station has multiple transmit antennas that emit signals to several users simultaneously. Each user also has multiple receive antennas. A base station measures the quality of transmission between each transmitter and receiver antennas. This is known as channel state information. The precoding problem consists of finding an appropriate weighting (phase and gain) of transmitting the signal in such a way that the signal power is maximized at the output of the receivers.

Here we have  $K$  users and for  $k$ -th user we would like to transmit him  $L_k$  symbols. Hence in total we would like to transmit a vector  $\mathbf{x} \in \mathbb{C}^L$ , where  $L = L_1 + \dots + L_K$ . First, we multiply the transmitted vector by a precoding matrix  $\mathbf{W} \in \mathbb{C}^{T \times L}$ , where  $T$  is a total number of transmit antennas on a base station. Then we transmit the precoded symbols to all the users. Suppose that  $k$ -th user has  $R_k$  receive antennas and  $\mathbf{H}_k \in \mathbb{C}^{R_k \times T}$  is a channel state information between  $k$ -th user antennas and antennas on the base station. Then  $k$ -th user receives  $\mathbf{H}_k \mathbf{W} \mathbf{x} + \mathbf{n}_k$ , where  $\mathbf{n}_k$  is a Gaussian noise, which appears as a result of thermal distortions of the system. Finally,  $k$ -th user applies a detection of transmitted symbols by multiplying the received vector by a detection matrix  $\mathbf{G}_k \in \mathbb{C}^{L_k \times R_k}$ . The final vector of detected symbols for all users is denoted by  $\mathbf{r} \in \mathbb{C}^L$ . The whole process of transmitting symbols is presented in Fig. 2. Note that the linear precoding and decoding are implemented by simple matrix multiplications.

Finally, the Multi-User MIMO model is described using the following linear system:

$$\mathbf{r} = \mathbf{G}(\mathbf{H}\mathbf{W}\mathbf{x} + \mathbf{n}). \quad (1)$$

Where  $\mathbf{r} \in \mathbb{C}^L$  is a received vector, and  $\mathbf{x} \in \mathbb{C}^L$  is a sent vector, and  $\mathbf{H} \in \mathbb{C}^{R \times T}$  is a channel matrix, and  $\mathbf{W} \in \mathbb{C}^{T \times L}$  is a precoding matrix, and  $\mathbf{G} \in \mathbb{C}^{L \times R}$  is a block-diagonal detection matrix, and  $\mathbf{n} \sim \mathcal{CN}(0, \mathbf{I}_L)$  is a noise-vector. The constant  $T$  is the number of transmit antennas,  $R$  is the total number of receive antennas, and  $L$  is the total number of transmitted symbols in the system. Usually they are related as  $L \leq R \leq T$ .

#### 3.1 Detection Matrix

*Detection* simulates the receiver on mobile devices. We study the most common form of the detection matrix  $\mathbf{G}$ , which is called Minimum MSE Interference Rejection Combine (*MMSE-IRC*) detection [18, 19]. It aims to reverse the channel to an identity matrix, and so *MMSE-IRC* receiver realizes the following rule, which requires solving a linear system at each iteration:

$$\mathbf{G}_k(\mathbf{H}_k, \mathbf{W}) = (\mathbf{H}_k \mathbf{W}_k)^H \left( \mathbf{H}_k \mathbf{W}_k (\mathbf{H}_k \mathbf{W}_k)^H + \mathbf{R}_{uu}^k(\mathbf{H}_k, \mathbf{W}_{\setminus k}) + \lambda \mathbf{I} \right)^{-1} \quad (2)$$

The matrix  $\mathbf{R}_{uu}^k$  related to unit symbol variance is calculated as follows:

$$\mathbf{R}_{uu}^k(\mathbf{H}_k, \mathbf{W}_{\setminus k}) = \mathbf{H}_k (\mathbf{W} \mathbf{W}^H - \mathbf{W}_k \mathbf{W}_k^H) \mathbf{H}_k^H = \mathbf{H}_k \left( \sum_{u=1, u \neq k}^K \mathbf{W}_u \mathbf{W}_u^H \right) \mathbf{H}_k^H \quad (3)$$

The scalar  $\lambda = \frac{\sigma^2}{P}$  is the system noise-to-signal ratio. The constant  $P$  refers to the base station power and  $\sigma^2$  refers to the system noise. Thus, we will consider the *noise* equal for all symbols:  $\mathbf{n} = \frac{\sigma^2}{P} \mathbf{1} \in \mathbb{C}^L$ , and detection  $\mathbf{G}$  which tends to eliminate it.

**Remark 1.** As written above  $\mathbf{H}_k \mathbf{W}_k (\mathbf{H}_k \mathbf{W}_k)^H + \mathbf{R}_{uu}^k = \mathbf{H}_k \mathbf{W} \mathbf{W}^H \mathbf{H}_k = \mathbf{\Omega}_k^{-1}$ , and so,  $\mathbf{G}_k(\mathbf{H}_k, \mathbf{W}) = (\mathbf{H}_k \mathbf{W}_k)^H \mathbf{\Omega}_k$

### 3.2 Quality Measures

The quality functions are based not on the actual sending symbols  $x \in \mathbb{C}^L$ , but on some distribution of them [1]. Thus, we get the common functions for all the assumed symbols, which can be sent using the specified precoding. The *Signal-to-Interference-and-Noise (SINR)* functional of the  $l = l(k)$ -th symbol and user  $k$  is defined as:

$$SINR_l(\mathbf{W}, \mathbf{H}_k, \mathbf{g}_l, \sigma, P) = \frac{|\mathbf{g}_l \mathbf{H}_k \mathbf{w}_l|^2}{\sum_{i \neq l} |\mathbf{g}_l \mathbf{H}_k \mathbf{w}_i|^2 + \|\mathbf{g}_l\|^2 \frac{\sigma^2}{P}}, \quad \forall l \in \mathcal{L}_k. \quad (4)$$

To get the formula for the  $k$ -th user *SINR*, namely the effective *SINR* and shows the signal quality of this user, we average all its  $L_k$  per-symbol *SINRs* (4) using the geometric mean:

$$SINR_k^{eff}(\mathbf{W}, \mathbf{H}_k, \mathbf{G}_k, \sigma, P) = \left( \prod_{l \in \mathcal{L}_k} SINR_l(\mathbf{W}, \mathbf{H}_k, \mathbf{g}_l, \sigma, P) \right)^{\frac{1}{L_k}} \quad (5)$$

Where the detection matrix  $\mathbf{G}_k \in \mathbb{C}^{L_k \times R_k}$  contains vector of the  $k$ -th user symbols  $\mathbf{g}_l$ . To get the final functional of *Spectral Efficiency* we apply the Shannon's formula over all effective user *SINRs* (5):

$$SE(\mathbf{W}, \mathbf{H}, \mathbf{G}, \sigma, P) = \sum_{k=1}^K L_k \log_2(1 + SINR_k^{eff}(\mathbf{W}, \mathbf{H}_k, \mathbf{G}_k, \sigma, P)) \rightarrow \max_{\mathbf{W}} \quad (6)$$

The formula (6) shows the throughput capacity of the system as a whole. Now it depends on the whole channel and detection matrices  $\mathbf{H} \in \mathbb{C}^{R \times T}$  and  $\mathbf{G} \in \mathbb{C}^{L \times R}$ . We will use it as our final score function, compare algorithms and find precoding matrices  $\mathbf{W} \in \mathbb{C}^{T \times L}$ , solving the problem of maximizing this function.

### 3.3 Power Constraints

We formulate the realistic [1] *per-antenna power constraints*. Since we have  $T$  equal transmitter antennas, the power limitation applied to each of them is  $\frac{P}{T}$ . The antenna power can be described in terms of the row norms of the precoding matrix:  $\|\mathbf{w}^m\|^2 \leq \frac{P}{T} \forall m$ .

It is clear that per-antenna constraints satisfies the total power:  $\|\mathbf{w}_1\| + \dots + \|\mathbf{w}^T\| \leq P$ , which is the *sum-power constraint* across all transmit antennas. While analytically attractive, such a *sum-power constraint* is often unrealistic in practice. In a physical implementation of a multi-antenna base station, each antenna has its own power amplifier in its analog front-end and is limited individually by the linearity of the power amplifier. Thus, a power constraint imposed on a *per-antenna basis* is more realistic.

## 4 Baseline Methods

The *precoding* matrix  $\mathbf{W}$  is responsible for the beamforming from the base station to the users. The baseline precoding algorithms do the following. Firstly, the baseline solutions obtain singular value decomposition for each user  $\mathbf{H}_k = \mathbf{U}_k^H \mathbf{S}_k \mathbf{V}_k \in \mathbb{C}^{R_k \times T}$  (Lemma 1) and take the first  $L_k$  singular vectors  $\tilde{\mathbf{V}}_k \in \mathbb{C}^{L_k \times T}$  which attend to the first  $L_k$  greatest singular values [20]. All these matrices are concatenated to the one matrix  $\mathbf{V} \in \mathbb{C}^{L \times T}$ , which is used as the main building block of the baseline precoding construction. Secondly, the precoding matrix is constructed from the obtained singular vectors. In the next sections, we describe the precoding matrix construction in the baseline methods.

We meet the power constraints using the scalar post-adjustment. We divide the precoding matrix on its maximal row norm  $\max\{\|\mathbf{w}^1\| \dots \|\mathbf{w}^T\|\}$  and scale them on  $\sqrt{\frac{P}{T}}$ . Thus, the per-antenna power constraints will satisfy  $\|\mathbf{w}^m\|^2 \leq \frac{P}{T} \forall m$ .

#### 4.1 Maximum-Ratio Transmission

The simplest way of computing the precoding matrix is to take the transpose conjugate of the channel singular vectors [12]:  $\mathbf{W}_{MRT} = \mu \mathbf{V}^H \mathbf{P} \in \mathbb{C}^{T \times L}$ , where matrix  $\mathbf{P} \in \mathbb{R}^{L \times L}$  denotes power allocation between symbols and constant  $\mu > 0$  utilizes the power constraints. In such a way, the signal beams will be sent directly to users without considering their interaction. The Maximum-Ratio approach is preferred in noisy systems where the noise power is higher than inter-user interference.

#### 4.2 Zero-Forcing

The next modification of the precoding algorithm performs decorrelation of the symbols using inverse correlation matrix of the channel vectors [13]:  $\mathbf{W}_{ZF} = \mu \mathbf{V}^H (\mathbf{V}\mathbf{V}^H)^{-1} \mathbf{P} \in \mathbb{C}^{T \times L}$  with matrix  $\mathbf{P} \in \mathbb{R}^{L \times L}$  and constant  $\mu > 0$ , which have the same meaning as in the previous section. Such precoding construction sends the signal beams to the users without creating any interference between them. Different from the previous method, the Zero-Forcing approach is preferred when the potential inter-user interference is higher than the noise power. There is a huge performance gain by eliminating the interference.

##### 4.2.1 Regularized Zero-Forcing

In the previous method, beams are sent not directly to the users but with some deviation, which actually reduces the payload. The following modification corrects the beams, which allows some inter-user interference and significantly increases the payload [14]:  $\mathbf{W}_{RZF} = \mu \mathbf{V}^H (\mathbf{V}\mathbf{V}^H + \mathbf{R})^{-1} \mathbf{P} \in \mathbb{C}^{T \times L}$  where diagonal matrix  $\mathbf{R} \in \mathbb{R}^{L \times L}$  denotes symbol *regularization* and matrix  $\mathbf{P} \in \mathbb{R}^{L \times L}$  and constant  $\mu > 0$  as the previous ones. As the baseline, we use a special form [21] of the regularization matrix  $\mathbf{R} = \frac{L\sigma^2}{P} \mathbf{I}$ . It is the most common precoding in real practice.

### 5 Precoding as Optimization Problem

We formulate the constrained smooth optimization problem:

$$\begin{aligned} & \underset{\mathbf{W} \in \mathbb{C}^{T \times L}}{\text{maximize}} && SE(\mathbf{W}, \mathbf{H}, \mathbf{G}, \sigma, P) \\ & \text{subject to} && \|\mathbf{w}^m\|^2 \leq \frac{P}{T}, \quad m = 1 \dots T \end{aligned} \quad (7)$$

Where  $\mathbf{w}^m \in \mathbb{C}^L$  in the  $m$ -th row of the precoding matrix.

#### 5.1 Conjugate Detection

It is convenient [20] to represent the user channel matrix  $k$  via its reduced Singular Value Decomposition (SVD):

$$\mathbf{H}_k = \mathbf{U}_k^H \mathbf{S}_k \mathbf{V}_k, \quad \mathbf{U}_k \mathbf{U}_k^H = \mathbf{U}_k^H \mathbf{U}_k = \mathbf{I}_{R_k}, \quad \mathbf{S}_k = \text{diag}\{s_1, \dots, s_{R_k}\}, \quad \mathbf{V}_k \mathbf{V}_k^H = \mathbf{I}_{R_k}. \quad (8)$$

Where the *channel matrix* for user  $k$ ,  $\mathbf{H}_k \in \mathbb{C}^{R_k \times T}$  contains channel vectors  $\mathbf{h}_i \in \mathbb{C}^T$  by rows, the singular values  $\mathbf{S}_k \in \mathbb{C}^{R_k \times R_k}$  are sorted by descending,  $\mathbf{U}_k \in \mathbb{C}^{R_k \times R_k}$  is a unitary matrix of left singular vectors, and matrix  $\mathbf{V}_k \in \mathbb{C}^{R_k \times T}$  consists of *right singular vectors*.

Collecting all users together, we can write the following decomposition:

**Lemma 1.** [22] Denote  $\mathbf{H} = [\mathbf{H}_1, \dots, \mathbf{H}_K] \in \mathbb{C}^{R \times T}$  the concatenation of individual channel rows  $\mathbf{H}_k$ . The following representation holds:

$$\mathbf{H} = \mathbf{U}^H \mathbf{S} \mathbf{V}. \quad (9)$$

where the  $\mathbf{H} \in \mathbb{C}^{R \times T}$ , and  $\mathbf{S} = \text{diag}(\mathbf{S}_k) \in \mathbb{C}^{R \times R}$ , and  $\mathbf{U} = \text{bdiag}(\mathbf{U}_k) \in \mathbb{C}^{R \times R}$  is block-diagonal unitary matrix, but  $\mathbf{V} = [\mathbf{V}_1, \dots, \mathbf{V}_K] \in \mathbb{C}^{R \times T}$  has a general form.

Conjugate Detection can be written in the following form:

$$\mathbf{G}^C := \tilde{\mathbf{S}}^{-1} \tilde{\mathbf{U}} \in \mathbb{C}^{L \times R}, \quad \mathbf{G}_k^C = \tilde{\mathbf{S}}_k^{-1} \tilde{\mathbf{U}}_k \in \mathbb{C}^{L_k \times R_k} \quad (10)$$

where  $\tilde{\mathbf{S}}_k \in \mathbb{C}^{L_k \times L_k}$  contains the first  $L_k$  largest singular values, and  $\tilde{\mathbf{U}}_k \in \mathbb{C}^{L_k \times R_k}$  contains the first  $L_k$  corresponding singular vectors.

**Theorem 1.** [22] Assuming (10), symbols  $\mathbf{x}$  of the system will flow only through the channel singular vectors  $\tilde{\mathbf{V}}$  as  $\mathbf{r} = \tilde{\mathbf{V}}\mathbf{W}\mathbf{x} + \tilde{\mathbf{S}}^{-1}\tilde{\mathbf{U}}\mathbf{n}$  since  $\mathbf{G}^C\mathbf{H} = \tilde{\mathbf{V}}$ .

*Proof.* Using Lemma (1) we can write

$$\mathbf{G}^C\mathbf{H} = \tilde{\mathbf{S}}^{-1}\tilde{\mathbf{U}}\mathbf{U}^H\mathbf{S}\mathbf{V} = \tilde{\mathbf{S}}^{-1}\left[ \mathbf{I} \mid \mathbf{O} \right]\mathbf{S}\mathbf{V} = \tilde{\mathbf{S}}^{-1}\left[ \begin{array}{c|c} \tilde{\mathbf{S}} & \mathbf{O} \\ \hline \mathbf{O} & \mathbf{O} \end{array} \right]\mathbf{V} = \tilde{\mathbf{S}}^{-1}\tilde{\mathbf{S}}\tilde{\mathbf{V}} = \tilde{\mathbf{V}}. \quad (11)$$

□

The conjugate and IRC detection matrices are very closely related to each other. We can use the conjugate detection at the base station to configure the precoding matrix assuming IRC for user equipments.

## 5.2 Approximated Functions

Assuming the conjugated detection  $\mathbf{G}^C$  (10) we have come to the following approximated function of the SINR:

$$\text{SINR}_l^C(\mathbf{W}, \tilde{\mathbf{v}}_l, s_l, \sigma^2, P) = \frac{|\tilde{\mathbf{v}}_l\mathbf{w}_l|^2}{\sum_{i \neq l}^L |\tilde{\mathbf{v}}_l\mathbf{w}_i|^2 + s_l^{-2}\frac{\sigma^2}{P}} \quad (12)$$

Spectral Efficiency function can be simplified in the following way:

$$\begin{aligned} \text{SE}^C(\mathbf{W}, \tilde{\mathbf{V}}, \mathbf{S}, \sigma, P) &= \sum_{l=1}^L \log_2(1 + \text{SINR}_l^C(\mathbf{W}, \tilde{\mathbf{v}}_l, s_l, \sigma, P)) = \\ &= \sum_{l=1}^L \log_2\left(\sum_{i=1}^L |\tilde{\mathbf{v}}_l\mathbf{w}_i|^2 + s_l^{-2}\frac{\sigma^2}{P}\right) - \sum_{l=1}^L \log_2\left(\sum_{i \neq l}^L |\tilde{\mathbf{v}}_l\mathbf{w}_i|^2 + s_l^{-2}\frac{\sigma^2}{P}\right) \rightarrow \max_{\mathbf{W}} \end{aligned} \quad (13)$$

Where  $\tilde{\mathbf{v}}_l \in \mathbb{C}^T$  is the singular vector of the  $l$ -th symbol, and  $s_l \in \mathbb{R}$  is the singular value of the  $l$ -th symbol.

One may notice that we have completely moved away from *user antennas* of shapes  $R_k$  and  $R$  and work only with *user layers* of shapes  $L_k$  and  $L$ . The formula now does not depend on channel matrix  $\mathbf{H}_k \in \mathbb{C}^{R_k \times T}$  but on the eigenvectors of the  $l$ -th layer  $\mathbf{v}_l \in \mathbb{C}^T$ , which has length  $T$  by the number of antennas. The inversed squared singular values  $s_l^{-2} \in \mathbb{R}$  scale the noise power.

Additionally, we consider the function of Single-User SINR for the  $k$ -th user:

$$\text{SUSINR}_k(\tilde{\mathbf{S}}_k, \sigma^2, P) := \frac{P}{L_k\sigma^2} \left( \prod_{l \in \mathcal{L}_k} s_l^2 \right)^{\frac{1}{L_k}}, \quad \text{AvSUSINR}(\tilde{\mathbf{S}}, \sigma^2, P) = \left( \prod_{k=1}^K \text{SUSINR}_k(\tilde{\mathbf{S}}_k, \sigma^2, P) \right)^{\frac{1}{K}}. \quad (14)$$

The formula (14) reflects the quality of the channel for the specified user without taking into account the others. It depends on the greatest  $L_k$  singular values  $\tilde{\mathbf{S}}_k \in \mathbb{R}^{L_k \times L_k}$  of the  $k$ -th user channel matrix  $\mathbf{H}_k \in \mathbb{C}^{R_k \times T}$  and can be derived from the (4) and (5) formulas assuming Single-User case, MRT or ZF Precoding matrix and Conjugate Detection (10). We will use this function in our experiments as a universal channel characteristic.

## 5.3 Proposed Optimization Solution

This method explicitly constrains antenna rows using (sub-)differentiable projection on a ball as a part of the Conjugate Spectral Efficiency function:

$$\underset{\mathbf{W} \in \mathbb{C}^{T \times L}}{\text{maximize}} \quad \text{SE}^C(\text{proj}_{P,T}(\mathbf{W}), \tilde{\mathbf{V}}, \mathbf{S}, \sigma, P) \quad (15)$$

$$\text{proj}_{P,T}(\mathbf{W}) = \begin{cases} \mathbf{w}^m, & \|\mathbf{w}^m\|^2 \leq \frac{P}{T} \\ \frac{\mathbf{w}^m}{\|\mathbf{w}^m\|} \sqrt{\frac{P}{T}}, & \|\mathbf{w}^m\|^2 > \frac{P}{T}, \quad \forall m = 1 \dots T \end{cases} \quad (16)$$

This parametrization achieves great performance in quality (see Tables 4, 5).

**Remark 2.** You can also use maximum row-norm projection  $\mu$ .

**Remark 3.** As the starting point, we are using Regularized Zero-Forcing  $\mathbf{W}_{RZF}$ .

---

**Algorithm 1:** On the optimal precoding matrix Quasi-Newton L-BFGS Scheme [15]

---

**Input:** Initial precoding matrix  $\mathbf{W}$ , channel singular vectors  $\tilde{\mathbf{V}}$ , channel singular values  $\mathbf{S}$ , station power  $P$ , noise  $\sigma^2$ , iterations  $N$   
Tolerance grad  $\varepsilon_g$ , termination tolerance on first order optimality (default: 1e-5);  
Tolerance change  $\varepsilon_c$ , termination tolerance on function value and parameter changes (default: 1e-9);

```

for  $t = 1$  to  $N$  do
  if True conditions on  $\varepsilon_g$  or  $\varepsilon_c$  then
    | return  $\text{proj}_{P,T}(\mathbf{W})$ 
  end
  Calculate the gradient:  $\nabla SE^C(\text{proj}_{P,T}(\mathbf{W}), \tilde{\mathbf{V}}, \mathbf{S}, \sigma, P)$ ;
  Find the optimal direction recursively:  $\mathbf{D} = \mathbf{D}(\nabla SE^C)$ ;
  Find the optimal step length  $\alpha = \arg \max_{\alpha} SE^C(\text{proj}_{P,T}(\mathbf{W} + \alpha \mathbf{D}))$ ;
  Make the optimization step:  $\mathbf{W} \leftarrow \mathbf{W} + \alpha \mathbf{D}$ ;
end
return  $\text{proj}_{P,T}(\mathbf{W})$ 

```

---

RZF	$SE^C(\mathbf{W})$	$\nabla SE^C(\mathbf{W})$	N-iterations of QNS
$x$	$x$	$x$	$\sim 3Nx$

Table 1: Relative computational complexity

#### 5.4 Relative Computational Complexity

The complexity of our algorithm is no more than  $\sim 3Nx$  times higher than the baseline *RZF*. On each iteration of *QNS* we have to compute gradient  $\nabla SE^C(\mathbf{W})$  of  $x$  complexity and adjust step length  $\alpha$ , which takes roughly two calls of the function  $SE^C(\mathbf{W})$  of  $2x$  total complexity (see the Table 1).

## 6 Numerical Experiments

We are testing the proposed approach in several scenarios generated using Quadriga [17] - open-source software for generating realistic radio channel impulse response. The main scenarios are 1) Rural Line-of-Sight 3GPP\_38.901\_RMa\_LOS, and 2) Urban Non-Line-of-Sight 3GPP\_38.901\_RMa\_NLOS [23]. For each scenario we generate 40 different channel matrices  $H \in \mathbb{C}^{n_{users} \times 4 \times 64}$ . The carrier frequency for each channel matrix is selected randomly over the bandwidth. User selection is described in the next section. The base station antenna array forms a grid with 8 placeholders along the  $y$  axis and 4 placeholders along the  $y$  axis. The receiver antenna array consists of two placeholders along the  $x$  axis. Each placeholder contains two cross-polarized antennas. An interested reader can find detailed hyperparameters for antenna models and generation processes in table 5 (see Appendix). All unlisted Quadriga parameters are those set by default. The main scenario is Urban Non-Line-of-Sight 3GPP 38.901 RMa NLOS.

For each scenario we generate 40 different channels:  $\mathbf{H} \in \mathbb{C}^{K \times R_k \times T}$ :

- $T = 64$  base station antennas,
- $R_k = 4$  user antennas,
- $L_k = 2$  user layers.

Scenario	Avg. Corr.
$K = 4$ Users	$7.6\% \pm 5.1\%$
$K = 8$ Users	$7.8\% \pm 3.6\%$

Table 2: Average absolute squared correlation between served users.

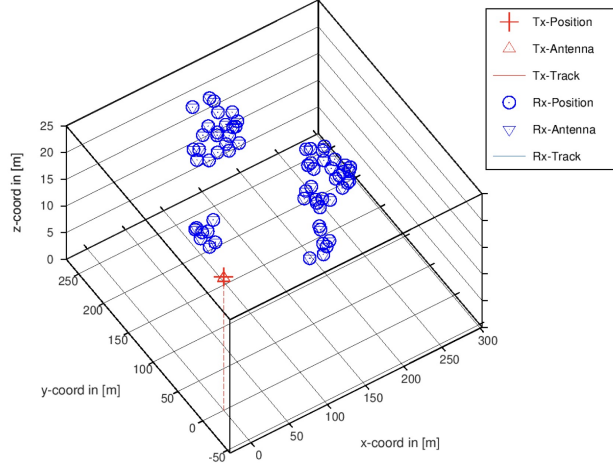


Figure 3: Example of Users for Urban Two Building Setup

### 6.1 Selecting user positions

For the Rural LOS scenario, we model users in the suburban landscape. We locate users on the ground, setting the height to 1.5m, and generate  $x, y$  positions uniformly in the  $120^\circ$  ray within 250m from the base station. For the NLOS scenario, we locate users in the urban landscape. Firstly, we sample up to 8 cluster centers  $x_c, y_c$  in the  $120^\circ$  ray from the base station within 2000m from the base station. Each cluster represents a part of a city building. We assign a random cluster height  $z_c = 1.5\text{m} + (3 \cdot U(\{1, \dots, 10\}) - 1)$ , selecting the cluster floor in a building from the uniform distribution  $U$ . Secondly, for each user, we assign a cluster id  $c(u)$  and sample  $x_u, y_u$  position randomly over the 60m circle around the cluster center. Thirdly, we sample the height of the user, given the height of the cluster, 80% of users we place at the floors near the cluster floor  $z_u = z_c(u) + 3 * U(\{-1, 0, 1\})$  m., and 20% of users we place outdoor  $z_u = 1.5\text{m}$ .

After generating channel matrices for a fairly large number of users (64), we select a subset of users, which are not too correlated, since too correlated users can be suited at a different time or frequency intervals. The correlation between users  $i, j$  is measured as squared cosine between the main singular vector:  $\cos^2(v_i, v_j) = |\langle \tilde{v}_{i0}, \tilde{v}_{j0} \rangle|^2$ . The statistics of mean correlations between all pairs of users served together (averaged over random seeds) are shown in the table 2. The Urban NLOS scenario is more challenging since on average, it provides more correlated users. We believe, our user generation produces realistic setups for both Urban and Rural cases and is simple to implement.

### 6.2 Quality Results

For each generated channel seed, we fix station power  $P = 1$  and select system noise  $\sigma^2$  for the specified  $AvSUSINR$  (14) average value (see table 2). We use binary search to select the noise  $\sigma^2$  since  $AvSUSINR$  depends on it monotonically. We report the hyper-parameters for Quadriga in the Table 5.

Both of our algorithms are superior to the baseline methods. The method Quasi-Newton Native works the best way since it optimizes the target function of (6) and directly solves the problem (7) using differentiable projection reduction. The method Quasi-Newton Simplified (QNS) solves the approximated problem (15) which requires less computational effort and is more tractable for the practice. Figures (4), (5) and tables (3), (4) contain the experimental results.

## 7 Conclusion

Multi-user Precoding optimization is a key problem in modern cellular wireless systems, which are based on massive MIMO technology. In this work, we propose a *QNS* algorithm, which achieves from 20% to 30% Spectral Efficiency gains comparing to the *RZF* baseline for the interesting *SUSINR* values. Our algorithm guarantees monotonic improvement of Spectral Efficiency value comparing to *RZF* for the whole *SUSINR* range. Using an optimization approach we can estimate the quality of given precoding relative to the optimal solution, i.e. estimate the quality upper bound. Finally, our algorithm can be simplified to further reduce computational complexity.



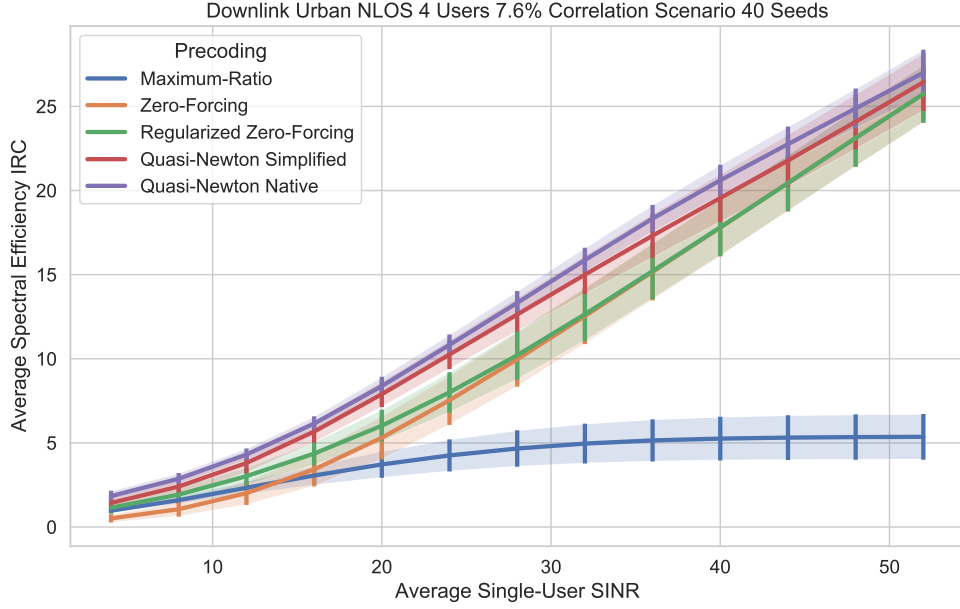


Figure 4: Urban NLOS 4 Users Numerical Results. The graph shows IRC Spectral Efficiency of the different Precoding algorithms in the *Urban NLOS* scenario. Proposal algorithms are Quasi-Newton Simplified and Quasi-Newton Native.

$SUSINR$	MR	ZF	RZF	QNS	QNS %
4	0.974	0.515	1.151	1.434	25
8	1.598	1.062	1.928	2.410	25
12	2.337	2.013	3.024	3.807	26
16	3.063	3.427	4.366	5.673	30
20	3.721	5.308	6.022	7.896	31
24	4.258	7.537	8.006	10.254	28
28	4.668	9.966	10.211	12.632	24
32	4.961	12.538	12.649	15.001	19
36	5.148	15.169	15.215	17.319	14
40	5.257	17.795	17.814	19.558	10
44	5.316	20.441	20.449	21.782	7
48	5.347	23.123	23.126	24.090	4
52	5.361	25.735	25.737	26.437	3

Table 3: Urban NLOS 4 Users *SE-IRC* Gains over RZF. The table shows IRC Spectral Efficiency of the different Precoding algorithms in the *Urban NLOS* scenario. The proposed algorithm is Quasi-Newton Simplified.

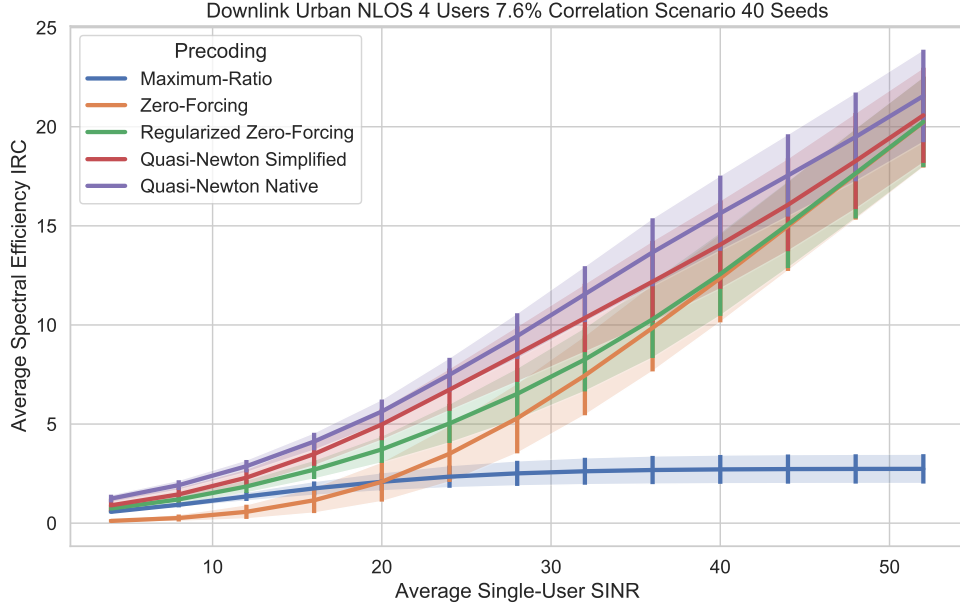


Figure 5: Urban NLOS 8 Users Numerical Results. The graph shows IRC Spectral Efficiency of the different Precoding algorithms in the *Urban NLOS* scenario. Proposal algorithms are Quasi-Newton Simplified and Quasi-Newton Native.

$SUSINR$	MR	ZF	RZF	QNS	QNS %
4	0.574	0.113	0.740	0.899	21
8	0.928	0.259	1.198	1.453	21
12	1.346	0.572	1.850	2.296	24
16	1.754	1.155	2.701	3.488	29
20	2.087	2.086	3.722	4.979	34
24	2.346	3.504	5.031	6.736	34
28	2.512	5.290	6.524	8.528	31
32	2.619	7.451	8.258	10.352	25
36	2.681	9.854	10.285	12.187	18
40	2.713	12.364	12.567	14.050	12
44	2.729	14.984	15.071	16.063	7
48	2.736	17.615	17.651	18.271	4
52	2.739	20.230	20.245	20.577	2

Table 4: Urban NLOS 8 Users *SE-IRC* Gains over RZF. The table shows IRC Spectral Efficiency of the different Precoding algorithms in the *Urban NLOS* scenario. The proposed algorithm is Quasi-Newton Simplified.

Parameter	Value
<b>Base station parameters</b>	
number of base stations	1
position, m: (x, y, z) axes	(0, 0, 25)
number of antenna placeholders (y axis)	8
number of antenna placeholders (z axis)	4
distance between placeholders (y axis)	0.5 wavelength
distance between placeholders (z axis)	1.7 wavelength
antenna model	3gpp-macro
half-Power in azimuth direction, deg	60
half-Power in elevation direction, deg	10
front-to back ratio, dB	20
total number of antennas	64
<b>Receiver parameters</b>	
number of placeholders at the receiver (x axis)	2
distance between placeholders (x axis)	0.5 wavelength
antenna model	half-wave-dipole
total number of antennas	4
<b>Quadriga simulation parameters</b>	
central band frequency	3.5 GHz
1 sample per meter (default value)	1
include delay of the LOS path	1
disable spherical waves (use_3GPP_baseline)	1
<b>Quadriga channel builders parameters</b>	
shadow fading sigma	0
cluster splitting	False
bandwidth	100 MHz
number of subcarriers	42

Table 5: Quadriga generation parameters

## References

- [1] Emil Björnson, Jakob Hoydis, and Luca Sanguinetti. Massive mimo networks: Spectral, energy, and hardware efficiency. *Foundations and Trends in Signal Processing*, 11(3-4):154–655, 2017.
- [2] Sergio Verdú. Spectral efficiency in the wideband regime. *IEEE Transactions on Information Theory*, 48(6):1319–1343, 2002.
- [3] Michael Joham, Wolfgang Utschick, and Josef A Nossek. Linear transmit processing in mimo communications systems. *IEEE Transactions on signal Processing*, 53(8):2700–2712, 2005.
- [4] Bernd Bandemer, Martin Haardt, and Samuli Visuri. Linear mmse multi-user mimo downlink precoding for users with multiple antennas. In *2006 IEEE 17th International Symposium on Personal, Indoor and Mobile Radio Communications*, pages 1–5. IEEE, 2006.
- [5] Giuseppe Caire and Shlomo Shamai. On the achievable throughput of a multiantenna gaussian broadcast channel. *IEEE Transactions on Information Theory*, 49(7):1691–1706, 2003.
- [6] Farrokh Rashid-Farrokhi, KJ Ray Liu, and Leandros Tassiulas. Transmit beamforming and power control for cellular wireless systems. *IEEE Journal on selected areas in communications*, 16(8):1437–1450, 1998.
- [7] Wei Yu and Tian Lan. Transmitter optimization for the multi-antenna downlink with per-antenna power constraints. *IEEE Transactions on signal processing*, 55(6):2646–2660, 2007.
- [8] Ami Wiesel, Yonina C Eldar, and Shlomo Shamai. Linear precoding via conic optimization for fixed mimo receivers. *IEEE transactions on signal processing*, 54(1):161–176, 2005.
- [9] Taesang Yoo and Andrea Goldsmith. Optimality of zero-forcing beamforming with multiuser diversity. In *IEEE International Conference on Communications, 2005. ICC 2005. 2005*, volume 1, pages 542–546. IEEE, 2005.

- [10] Federico Boccardi and Howard Huang. Optimum power allocation for the mimo-bc zero-forcing precoder with per-antenna power constraints. In *2006 40th Annual Conference on Information Sciences and Systems*, pages 504–504. IEEE, 2006.
- [11] Quentin H Spencer, A Lee Swindlehurst, and Martin Haardt. Zero-forcing methods for downlink spatial multiplexing in multiuser mimo channels. *IEEE transactions on signal processing*, 52(2):461–471, 2004.
- [12] Titus KY Lo. Maximum ratio transmission. In *1999 IEEE international conference on communications (Cat. No. 99CH36311)*, volume 2, pages 1310–1314. IEEE, 1999.
- [13] Taesang Yoo and Andrea Goldsmith. On the optimality of multiantenna broadcast scheduling using zero-forcing beamforming. *IEEE Journal on selected areas in communications*, 24(3):528–541, 2006.
- [14] Zijian Wang and Wen Chen. Regularized zero-forcing for multiantenna broadcast channels with user selection. *IEEE Wireless Communications Letters*, 1(2):129–132, 2012.
- [15] Ciyou Zhu, Richard H Byrd, Peihuang Lu, and Jorge Nocedal. Algorithm 778: L-bfgs-b: Fortran subroutines for large-scale bound-constrained optimization. *ACM Transactions on mathematical software (TOMS)*, 23(4):550–560, 1997.
- [16] Adam Paszke, Sam Gross, Soumith Chintala, Gregory Chanan, Edward Yang, Zachary DeVito, Zeming Lin, Alban Desmaison, Luca Antiga, and Adam Lerer. Automatic differentiation in pytorch. 2017.
- [17] Stephan Jaeckel, Leszek Raschkowski, Kai Börner, and Lars Thiele. Quadriga: A 3-d multi-cell channel model with time evolution for enabling virtual field trials. *IEEE Transactions on Antennas and Propagation*, 62(6):3242–3256, 2014.
- [18] Dirk Wubben, Ronald Bohnke, Volker Kuhn, and K-D Kammeyer. Near-maximum-likelihood detection of mimo systems using mmse-based lattice-reduction. In *2004 IEEE International Conference on Communications (IEEE Cat. No. 04CH37577)*, volume 2, pages 798–802. IEEE, 2004.
- [19] Bin Ren, Yingmin Wang, Shaohui Sun, Yawen Zhang, Xiaoming Dai, and Kai Niu. Low-complexity mmse-irc algorithm for uplink massive mimo systems. *Electronics Letters*, 53(14):972–974, 2017.
- [20] Liang Sun and Matthew R McKay. Eigen-based transceivers for the mimo broadcast channel with semi-orthogonal user selection. *IEEE Transactions on Signal Processing*, 58(10):5246–5261, 2010.
- [21] Christian B Peel, Bertrand M Hochwald, and A Lee Swindlehurst. A vector-perturbation technique for near-capacity multiantenna multiuser communication-part i: channel inversion and regularization. *IEEE Transactions on Communications*, 53(1):195–202, 2005.
- [22] Evgeny Bobrov, Boris Chinyaev, Viktor Kuznetsov, Hao Lu, Dmitrii Minenkov, Sergey Troshin, Daniil Yudakov, and Danila Zaev. Adaptive regularized zero-forcing beamforming in massive mimo with multi-antenna users. *arXiv preprint arXiv:2107.00853*, 2021.
- [23] Frode Bohagen, Pål Orten, and GE Oien. Construction and capacity analysis of high-rank line-of-sight mimo channels. In *IEEE Wireless Communications and Networking Conference, 2005*, volume 1, pages 432–437. IEEE, 2005.